

Coordinated Expansion Planning of Natural Gas and Electric Power Systems

Bining Zhao, *Student Member, IEEE*, Antonio J. Conejo, *Fellow, IEEE*, and Ramteen Sioshansi, *Senior Member, IEEE*

Abstract—The interdependency between natural gas and electric power systems is becoming increasingly tight as the share of natural gas-fired generators increases. Within this context, this paper addresses the coordinated expansion planning of natural gas and power systems. We analyze the trade-off of building natural gas-related and other facilities. We use a two-stage stochastic optimization model that provides an appropriate balance between accuracy and computational tractability and represents uncertainty pertaining to electricity and natural gas demands. We analyze the functioning of the model through a small example and a case study based on the IEEE 118-bus system.

Index Terms—Power system planning, natural gas, stochastic optimization

I. INTRODUCTION

THE interdependency between natural gas and power systems is becoming tighter as the share of natural gas-fired generators increases. This interdependency is especially relevant if natural gas supplies are uncertain. Supply uncertainty may be caused by natural gas being prioritized for heating, as opposed to electricity production [1].

Within this context, we address the coordinated expansion planning of a natural gas and power system with the purpose of optimally allocating available natural gas resources. Such coordinated expansion planning can prevent electricity-supply disruptions due to limited natural gas (e.g., during extreme-weather events). The model that we propose can analyze the trade-offs between building natural gas-related and other facilities. Our model is static, inasmuch as it considers a single planning stage followed by operating periods. This yields a two-stage stochastic optimization model, wherein the first stage is the planning stage, during which all investment decisions are made. The second stage is the operating stage, during which operating decisions are made under different demand-growth rates and operating conditions. This model structure provides an appropriate balance between accuracy and computational tractability. To clearly show the interactions between natural gas and power systems, which is our focus, we only consider natural gas- and electricity-demand growth

This work was supported by NSF grant 1548015.

B. Zhao is with the Department of Electrical and Computer Engineering, The Ohio State University, Columbus, OH 43210, USA (e-mail: zhao.1418@osu.edu).

A. J. Conejo is with the Departments of Integrated Systems Engineering and Electrical and Computer Engineering, The Ohio State University, Columbus, OH 43210, USA (e-mail: conejonavarro.1@osu.edu).

R. Sioshansi is with the Department of Integrated Systems Engineering, The Ohio State University, Columbus, OH 43210, USA (e-mail: sioshansi.1@osu.edu).

rates as being uncertain. Although we neglect other sources of uncertainty, such as renewable generation, they can be easily incorporated into the proposed modeling framework. We illustrate the model using a simple eight-zone ISO New England test system and the IEEE 118-bus system [2].

The existing literature takes a number of approaches to modeling the joint expansion of natural gas and power systems. Unsihuay-Vila *et al.* [3] use a deterministic, linear, multistage model. Qiu *et al.* [4] use Taylor series approximations and piecewise linear functions to represent the physical properties of natural gas and power systems in expansion planning. Saldarriaga *et al.* [5] propose a holistic approach to solving a mixed-integer nonlinear model that coordinates planning of natural gas and electricity distribution networks. Qiu *et al.* [6] and Barati *et al.* [7] develop deterministic multistage nonlinear expansion models, which they solve using metaheuristic algorithms. Qiu *et al.* [6] also conduct a ‘robustness check,’ in which the operations of the resulting system under different conditions are examined. Zhang *et al.* [8] propose a joint planning model that emphasizes power system security and reliability. Chaudry *et al.* [9] and Qiu *et al.* [10] develop models to achieve a low-carbon energy system through joint planning of power and natural gas systems. Wang *et al.* [11] develop a coordinated planning model for natural gas and power systems that considers uncertainties. However, their problem is solved by applying a modified differential evolution method to the two systems separately and iteratively. Jin and Ryan [12] propose a bi-level fuel-supply and power-system investment model, which can be used to study the effect of investment decisions on the welfare of fuel suppliers, generation companies, and consumers. Sharan and Balasubramanian [13] develop a generation and transmission planning model that considers fuel-transportation constraints. Bistline [14], [15] investigates the influence of uncertainties related to natural gas prices and climate policies on power system investment.

Our work makes two contributions to this existing literature. First, our model uses a two-stage stochastic optimization framework to represent uncertainty in natural gas and electricity demand growth. Thus, our model is effective in analyzing the trade-offs between building natural gas and other facilities, including natural gas pipelines, natural gas-fired units, and other thermal units. Secondly, we apply our model to case studies to comprehensively analyze these trade-offs between different types of facilities and to derive policy conclusions.

The application of stochastic optimization to energy-system planning is not novel. However, there is not, to our knowledge, any existing literature that applies these methods to

coordinated expansion planning of natural gas and power systems. Rather, the existing literature either employs deterministic models (which do not capture uncertainties), uses metaheuristics or other approximation algorithms (which do not guarantee optimal solutions) to solve the models, or only considers investments in part of the system (e.g., power system investments only, with representation of fuel-related constraints).

The remainder of this paper is organized as follows. Section II describes the proposed two-stage stochastic optimization model. Section III demonstrates the model through a simple example, while Section IV studies a more comprehensive case study based on the IEEE 118-bus system. Section V concludes.

II. MODEL FORMULATION

We provide a detailed formulation of our proposed model.

A. Notation

We begin by introducing the following model notation.

Sets and Indices

	Parameters
g	b_g^E heat rate of existing natural gas-fired unit g [MBTU/MWh]
k	b_k^C heat rate of candidate natural gas-fired unit k [MBTU/MWh]
m, n	$B_{m,n}$ susceptance of existing transmission line connecting nodes m and n [p.u.]
	$\hat{B}_{m,n}$ susceptance of candidate transmission line connecting nodes m and n [p.u.]
k	c_k^{GC} operation and maintenance cost of candidate natural gas-fired unit k [\$/MWh]
g	c_g^{GE} operation and maintenance cost of existing natural gas-fired unit g [\$/MWh]
j	c_j^{TC} marginal cost of candidate thermal unit j [\$/MWh]
	c_i^{TE} marginal cost of existing thermal unit i [\$/MWh]
k	$C_k^{G,INV}$ investment cost of candidate natural gas-fired unit k [\$/MW]
j	$C_j^{T,INV}$ investment cost of candidate thermal unit i [\$/MW]
m, n	$C_{m,n}^{C,INV}$ investment cost of candidate transmission line connecting nodes m and n [\\$]
p, q	$C_{p,q}^{P,INV}$ investment cost of candidate natural gas pipeline connecting nodes p and q [\$/MBTU/h]
p	D_p reference non-generation-related natural gas load at natural gas node p [MBTU/h]
m, n	$F_{m,n}^{\max}$ capacity of existing transmission line connecting nodes m and n [MW]
o	$F_{m,n}^{C,\max}$ capacity of candidate transmission line connecting nodes m and n [MW]
ω	$f_{\omega,o}^{EL}$ electric load in operating condition o of scenario ω [p.u.]
n	$f_{\omega,o}^{GD}$ non-generation-related gas load in operating condition o of scenario ω [p.u.]
ω	L_n reference electric load at power system node n [MW]
Φ_n^{GC}	M large constant
Φ_n^{GE}	N reference power system node
Φ_n^{TC}	$P_k^{GC,INV,\max}$ maximum capacity of candidate natural gas-fired unit k that can be built [MW]
Φ_n^{TE}	$P_g^{GE,\max}$ capacity of existing natural gas-fired unit g [MW]
Λ_n	$P_j^{TC,INV,\max}$ maximum capacity of candidate thermal unit j that can be built [MW]
$\hat{\Lambda}_n$	$P_i^{TE,\max}$ capacity of existing thermal unit i [MW]
Ξ_p	$Q_{p,q}^{\max}$ capacity of existing natural gas pipeline connecting nodes p and q [MBTU/h]
$\hat{\Xi}_p$	$Q_{p,q}^{INV,\max}$ maximum capacity of natural gas pipeline connecting nodes p and q that can be added [MBTU/h]
Ξ_p^{GE}	S_p^{\max} maximum natural gas available at node p [MBTU/h]
Ξ_p^{GC}	$V^{LL,E}$ value of lost electric load [\$/MWh]
	$V^{LL,G}$ value of lost natural gas load [\$/MBTU]
	W_o weight of operating condition o [h]
	$\beta_{p,o}$ node- p natural gas price in operating condition o [\$/MBTU]
	ρ_ω probability of scenario ω

Variables

$P_k^{\text{GC,INV}}$	capacity of candidate natural gas-fired unit k built [MW]
$P_j^{\text{TC,INV}}$	capacity of candidate thermal unit j built [MW]
$x_{m,n}$	binary variable that equals 1 if candidate transmission line connecting nodes m and n is built, equals 0 otherwise
$\hat{Q}_{p,q}^{\text{INV}}$	capacity of candidate natural gas pipeline connecting nodes p and q built [MBTU/h]
$F_{m,n,\omega,o}^{\text{C}}$	power flow through candidate transmission line connecting nodes m and n in operating condition o of scenario ω [MW]
$L_{n,\omega,o}^{\text{shed}}$	unserved electric energy at node n in operating condition o of scenario ω [MW]
$P_{k,\omega,o}^{\text{GC}}$	production of candidate natural gas-fired unit k in operating condition o of scenario ω [MW]
$P_{g,\omega,o}^{\text{GE}}$	production of existing natural gas-fired unit g in operating condition o of scenario ω [MW]
$P_{j,\omega,o}^{\text{TC}}$	production of candidate thermal unit j in operating condition o of scenario ω [MW]
$P_{i,\omega,o}^{\text{TE}}$	production of existing thermal unit i in operating condition o of scenario ω [MW]
$\theta_{n,\omega,o}$	phase angle of power system node n in operating condition o of scenario ω [rad]
$D_{p,\omega,o}^{\text{shed}}$	unserved natural gas demand at node p in operating condition o of scenario ω [MBTU]
$Q_{p,q,\omega,o}$	natural gas flow through existing pipeline connecting nodes p and q in operating condition o of scenario ω [MBTU/h]
$\hat{Q}_{p,q,\omega,o}$	natural gas flow through candidate pipeline connecting nodes p and q in operating condition o of scenario ω [MBTU/h]
$Q_{k,\omega,o}^{\text{GC}}$	fuel usage of candidate natural gas-fired unit k in operating condition o of scenario ω [MBTU/h]
$Q_{g,\omega,o}^{\text{GE}}$	fuel usage of existing natural gas-fired unit g in operating condition o of scenario ω [MBTU/h]
$S_{p,\omega,o}$	natural gas extracted from node p in operating condition o of scenario ω [MBTU/h]

B. Optimization Model

The model is formulated as:

$$\begin{aligned}
 \min \sum_{k \in \Phi^{\text{GC}}} C_k^{\text{GC}} P_k^{\text{GC,INV}} + \sum_{j \in \Phi^{\text{TC}}} C_j^{\text{TC}} P_j^{\text{TC,INV}} \\
 + \sum_{n \in \Lambda, m \in \hat{\Lambda}_n} x_{m,n} C_{m,n}^{\text{INV}} + \sum_{p \in \Xi, q \in \hat{\Xi}_p} C_{p,q}^{\text{P,INV}} \hat{Q}_{p,q}^{\text{INV}} \\
 + \sum_{\omega \in \Omega, o \in O} \rho_\omega W_o \cdot \left\{ \sum_{g \in \Phi^{\text{GE}}} c_g^{\text{GE}} P_{g,\omega,o}^{\text{GE}} \right. \\
 + \sum_{i \in \Phi^{\text{TE}}} c_i^{\text{TE}} P_{i,\omega,o}^{\text{TE}} + \sum_{k \in \Phi^{\text{GC}}} c_k^{\text{GC}} P_{k,\omega,o}^{\text{GC}} \\
 \left. + \sum_{j \in \Phi^{\text{TC}}} c_j^{\text{TC}} P_{j,\omega,o}^{\text{TC}} + \sum_{n \in \Lambda} V^{\text{LL,E}} L_{n,\omega,o}^{\text{shed}} \right\}
 \end{aligned}$$

$$\begin{aligned}
 & + \sum_{p \in \Xi} \left[V^{\text{LL,G}} D_{p,\omega,o}^{\text{shed}} + \beta_{p,o} \cdot \left(\sum_{g \in \Xi_p^{\text{GE}}} Q_{g,\omega,o}^{\text{GE}} \right. \right. \\
 & \left. \left. + \sum_{k \in \Xi_p^{\text{GC}}} Q_{k,\omega,o}^{\text{GC}} \right) \right] \right\} \quad (1)
 \end{aligned}$$

$$\text{s.t. } 0 \leq P_k^{\text{GC,INV}} \leq P_k^{\text{GC,INV,max}}; \forall k \in \Phi^{\text{GC}}; \quad (2)$$

$$0 \leq P_j^{\text{TC,INV}} \leq P_j^{\text{TC,INV,max}}; \forall j \in \Phi^{\text{TC}}; \quad (3)$$

$$x_{m,n} \in \{0, 1\}; \forall n \in \Lambda, m \in \hat{\Lambda}_n; \quad (4)$$

$$0 \leq \hat{Q}_{p,q}^{\text{INV}} \leq Q_{p,q}^{\text{INV,max}}; \forall p \in \Xi, q \in \hat{\Xi}_p; \quad (5)$$

$$\begin{aligned}
 \sum_{i \in \Phi^{\text{TE}}} P_{i,\omega,o}^{\text{TE}} + \sum_{g \in \Phi^{\text{GE}}} P_{g,\omega,o}^{\text{GE}} + \sum_{j \in \Phi^{\text{TC}}} P_{j,\omega,o}^{\text{TC}} + \sum_{k \in \Phi^{\text{GC}}} P_{k,\omega,o}^{\text{GC}} \\
 - f_{\omega,o}^{\text{EL}} L_n + L_{n,\omega,o}^{\text{shed}} = \sum_{m \in \Lambda_n} B_{m,n} \cdot (\theta_{n,\omega,o} - \theta_{m,\omega,o})
 \end{aligned}$$

$$+ \sum_{m \in \hat{\Lambda}_n} F_{m,n,\omega,o}^{\text{C}}; \forall n \in \Lambda, \omega \in \Omega, o \in O; \quad (6)$$

$$- F_{m,n}^{\text{max}} \leq B_{m,n} \cdot (\theta_{n,\omega,o} - \theta_{m,\omega,o}) \leq F_{m,n}^{\text{max}}; \quad (7)$$

$$\forall n \in \Lambda, m \in \Lambda_n, \omega \in \Omega, o \in O;$$

$$- F_{m,n}^{\text{C,max}} x_{m,n} \leq F_{m,n,\omega,o}^{\text{C}} \leq F_{m,n}^{\text{C,max}} x_{m,n}; \quad (8)$$

$$\forall n \in \Lambda, m \in \hat{\Lambda}_n, \omega \in \Omega, o \in O;$$

$$- (1 - x_{m,n}) M \leq F_{m,n,\omega,o}^{\text{C}} - \hat{B}_{m,n} \cdot (\theta_{n,\omega,o} - \theta_{m,\omega,o}) \\
 \leq (1 - x_{m,n}) M; \quad (9)$$

$$\forall n \in \Lambda, m \in \hat{\Lambda}_n, \omega \in \Omega, o \in O;$$

$$\theta_{N,\omega,o} = 0; \forall \omega \in \Omega, o \in O; \quad (10)$$

$$-\pi \leq \theta_{n,\omega,o} \leq \pi; \forall n \in \Lambda, \omega \in \Omega, o \in O; \quad (11)$$

$$0 \leq L_{n,\omega,o}^{\text{shed}} \leq f_{\omega,o}^{\text{EL}} L_n; \forall n \in \Lambda, \omega \in \Omega, o \in O; \quad (12)$$

$$0 \leq P_{k,\omega,o}^{\text{GC}} \leq P_k^{\text{GC,INV}}; \forall k \in \Phi^{\text{GC}}, \omega \in \Omega, o \in O; \quad (13)$$

$$0 \leq P_{g,\omega,o}^{\text{GE}} \leq P_g^{\text{GE,max}}; \forall g \in \Phi^{\text{GE}}, \omega \in \Omega, o \in O; \quad (14)$$

$$0 \leq P_{j,\omega,o}^{\text{TC}} \leq P_j^{\text{TC,INV}}; \forall j \in \Phi^{\text{TC}}, \omega \in \Omega, o \in O; \quad (15)$$

$$0 \leq P_{i,\omega,o}^{\text{TE}} \leq P_i^{\text{TE,max}}; \forall i \in \Phi^{\text{TE}}, \omega \in \Omega, o \in O; \quad (16)$$

$$S_{p,\omega,o} - f_{\omega,o}^{\text{GD}} D_p + D_{p,\omega,o}^{\text{shed}} - \sum_{g \in \Xi_p^{\text{GE}}} Q_{g,\omega,o}^{\text{GE}} \quad (17)$$

$$- \sum_{k \in \Xi_p^{\text{GC}}} Q_{k,\omega,o}^{\text{GC}} = \sum_{q \in \Xi_p} Q_{p,q,\omega,o} + \sum_{q \in \hat{\Xi}_p} \hat{Q}_{p,q,\omega,o}; \quad \forall p \in \Xi, \omega \in \Omega, o \in O;$$

$$0 \leq S_{p,\omega,o} \leq S_p^{\text{max}}; \forall p \in \Xi, \omega \in \Omega, o \in O; \quad (18)$$

$$- \hat{Q}_{p,q}^{\text{INV}} \leq \hat{Q}_{p,q,\omega,o} \leq \hat{Q}_{p,q}^{\text{INV}}; \quad (19)$$

$$\forall p \in \Xi, q \in \hat{\Xi}_p, \omega \in \Omega, o \in O;$$

$$- Q_{p,q}^{\text{max}} \leq Q_{p,q,\omega,o} \leq Q_{p,q}^{\text{max}}; \quad (20)$$

$$\forall p \in \Xi, q \in \Xi_p, \omega \in \Omega, o \in O;$$

$$0 \leq D_{p,\omega,o}^{\text{shed}} \leq f_{\omega,o}^{\text{GD}} D_p; \forall p \in \Xi, \omega \in \Omega, o \in O; \quad (21)$$

$$Q_{k,\omega,o}^{\text{GC}} = b_k^{\text{GC}} P_{k,\omega,o}^{\text{GC}}; \forall k \in \Xi_p^{\text{GC}}, \omega \in \Omega, o \in O; \quad (22)$$

$$Q_{g,\omega,o}^{\text{GE}} = b_g^{\text{GE}} P_{g,\omega,o}^{\text{GE}}; \forall g \in \Xi_p^{\text{GE}}, \omega \in \Omega, o \in O. \quad (23)$$

Our model is formulated as a static investment problem [16], in which a single set of investment decisions are initially made. These are then followed by operating decisions under different uncertain scenarios (ω) and operating conditions (o).

The scenarios describe long-term uncertainties (*i.e.*, electricity and natural gas demand growth), while the operating conditions describe short-term variability (*i.e.*, hourly, diurnal, and seasonal electricity and natural gas demand patterns) [17]. The proposed model is a mixed-integer linear stochastic problem, which can be solved using a standard software package (*e.g.*, CPLEX).

Objective function (1) minimizes the sum of expected operation and investment costs. The first four terms of the objective function are, respectively, the investment costs of candidate natural gas-fired units, thermal units, transmission lines, and natural gas pipelines. The remaining terms represent the expected operation cost of the two systems. Natural gas-fired units incur two types of operating costs: (i) fuel and (ii) operation and maintenance costs. Fuel cost is computed by multiplying fuel use by the natural gas price. This fuel cost is the last term in objective function (1).

The model has two types of constraints. Constraints (2)–(5) pertain to the investment stage while the remaining are associated with operating decisions. Constraints (6)–(16) and (17)–(21) relate to the operation of the power and natural gas systems, respectively, and constraints (22) and (23) ‘link’ the two systems together via the fuel use of natural gas-fired units.

Constraints (2) and (3) impose limits on natural gas-fired and thermal unit capacity that can be built. Constraints (4) model transmission line investments as binary decisions. Constraints (5) impose limits on natural gas pipeline capacity that can be added to existing pipelines or that can be installed in new pipelines.

Constraints (6)–(16) impose operating restrictions on the power system. Constraints (6) impose nodal electric load balance. Constraints (7) and (8) impose flow limits on existing and candidate transmission lines, respectively. Constraints (9) define flows on candidate transmission lines that are built, and fixes flows equal to zero for lines that are not built. Constraints (10) set the reference node’s phase angle equal to zero while constraints (11) bound the phase angles of other nodes. Constraints (12) limit the amount of load shed in the power system to be less than the actual load. Constraints (13)–(16) impose production limits on existing and candidate natural gas-fired and thermal units.

Constraints (17)–(21) impose operating restrictions on the natural gas system. Constraints (17) impose nodal natural gas load balance. Constraints (18) bound the amount of fuel that can be extracted from each natural gas node (*i.e.*, wells and other natural gas sources). Constraints (19) and (20) impose flow limits on candidate and existing natural gas pipelines, respectively. Our model employs a linearized natural gas pipeline model (*i.e.*, a transport model). Although some works employ nonlinear models of natural gas flows, we opt to employ a simpler linear model. Our main reason for this choice is computational complexity. A nonlinear flow model would result in our having a mixed-integer nonlinear stochastic optimization problem, which would raise tractability issues. We believe that linear flows provide a sufficient level of detail for the type of planning exercise that our model focuses on. Indeed, many of the works employing nonlinear flows focus on operation as opposed to planning. Moreover, planning models

that represent nonlinear flows are typically deterministic and do not capture uncertainties [5]–[7]. Constraints (21) limit the amount of load shed in the gas system to be less than the actual non-generation-related load.

Finally, constraints (22) and (23) define the fuel usage of candidate and existing natural gas-fired units, respectively. These constraints link the two systems together. For sake of simplicity, we assume a linear relationship between fuel usage and power production (*i.e.*, a fixed heat rate) for all natural gas-fired units. Fuel usage could easily be modeled using piecewise-linear functions (which is often used to represent part-load efficiency effects), with little increase in computational complexity.

C. Value of Stochastic Solution

One way that we demonstrate the benefit of our proposed planning model is by computing the value of stochastic solution (VSS). VSS estimates the benefit of explicitly modeling uncertainties when making first-stage investment decisions [18].

To define the VSS, we first formulate a deterministic variant of the model that is introduced in Section II-B. Uncertain natural gas and electric loads, $f_{\omega,o}^{\text{EL}}$ and $f_{\omega,o}^{\text{GD}}$, are replaced by their expected values:

$$\bar{f}_o^{\text{EL}} = \sum_{\omega \in \Omega} \rho_{\omega} f_{\omega,o}^{\text{EL}},$$

and:

$$\bar{f}_o^{\text{GD}} = \sum_{\omega \in \Omega} \rho_{\omega} f_{\omega,o}^{\text{GD}},$$

in this deterministic model, which is formulated as:

$$\begin{aligned} \min \sum_{k \in \Phi^{\text{GC}}} C_k^{\text{GC}} P_k^{\text{GC,INV}} + \sum_{j \in \Phi^{\text{TC}}} C_j^{\text{TC}} P_j^{\text{TC,INV}} \\ + \sum_{n \in \Lambda, m \in \hat{\Lambda}_n} x_{m,n} C_{m,n}^{\text{C,INV}} + \sum_{p \in \Xi, q \in \hat{\Xi}_p} C_{p,q}^{\text{P,INV}} \hat{Q}_{p,q}^{\text{INV}} \\ + \sum_{o \in O} W_o \cdot \left\{ \sum_{g \in \Phi^{\text{GE}}} c_g^{\text{GE}} P_{g,o}^{\text{GE}} + \sum_{i \in \Phi^{\text{TE}}} c_i^{\text{TE}} P_{i,o}^{\text{TE}} \right. \\ + \sum_{k \in \Phi^{\text{GC}}} c_k^{\text{GC}} P_{k,o}^{\text{GC}} + \sum_{j \in \Phi^{\text{TC}}} c_j^{\text{TC}} P_{j,o}^{\text{TC}} + \sum_{n \in \Lambda} V^{\text{LL,E}} L_{n,o}^{\text{shed}} \\ + \sum_{p \in \Xi} \left[V^{\text{LL,G}} D_{p,o}^{\text{shed}} + \beta_{p,o} \cdot \left(\sum_{g \in \Xi_p^{\text{GE}}} Q_{g,o}^{\text{GE}} \right. \right. \\ \left. \left. + \sum_{k \in \Xi_p^{\text{GC}}} Q_{k,o}^{\text{GC}} \right) \right] \right\} \end{aligned} \quad (24)$$

$$\text{s.t. } 0 \leq P_k^{\text{GC,INV}} \leq P_k^{\text{GC,INV,max}}; \forall k \in \Phi^{\text{GC}}; \quad (25)$$

$$0 \leq P_j^{\text{TC,INV}} \leq P_j^{\text{TC,INV,max}}; \forall j \in \Phi^{\text{TC}}; \quad (26)$$

$$x_{m,n} \in \{0, 1\}; \forall n \in \Lambda, m \in \hat{\Lambda}_n; \quad (27)$$

$$0 \leq \hat{Q}_{p,q}^{\text{INV}} \leq Q_{p,q}^{\text{INV,max}}; \forall p \in \Xi, q \in \hat{\Xi}_p; \quad (28)$$

$$\sum_{i \in \Phi_n^{\text{TE}}} P_{i,o}^{\text{GE}} + \sum_{g \in \Phi_n^{\text{GE}}} P_{g,o}^{\text{GE}} + \sum_{j \in \Phi_n^{\text{TC}}} P_{j,o}^{\text{TC}} + \sum_{k \in \Phi_n^{\text{GC}}} P_{k,o}^{\text{GC}}$$

$$\begin{aligned} -\bar{f}_o^{\text{EL}} L_n + L_{n,o}^{\text{shed}} &= \sum_{m \in \Lambda_n} B_{m,n} \cdot (\theta_{n,o} - \theta_{m,o}) \\ &+ \sum_{m \in \hat{\Lambda}_n} F_{m,n,o}^{\text{C}}; \forall n \in \Lambda, o \in O; \end{aligned} \quad (29)$$

$$\begin{aligned} -F_{m,n}^{\max} &\leq B_{m,n} \cdot (\theta_{n,o} - \theta_{m,o}) \leq F_{m,n}^{\max}; \\ &\forall n \in \Lambda, m \in \Lambda_n, o \in O; \end{aligned} \quad (30)$$

$$\begin{aligned} -F_{m,n}^{\text{C},\max} x_{m,n} &\leq F_{m,n}^{\text{C}} \leq F_{m,n}^{\text{C},\max} x_{m,n}; \\ &\forall n \in \Lambda, m \in \hat{\Lambda}_n, o \in O; \end{aligned} \quad (31)$$

$$\begin{aligned} -(1-x_{m,n})M &\leq F_{m,n,o}^{\text{C}} - \hat{B}_{m,n} \cdot (\theta_{n,o} - \theta_{m,o}) \\ &\leq (1-x_{m,n})M; \forall n \in \Lambda, m \in \hat{\Lambda}_n, o \in O; \end{aligned} \quad (32)$$

$$\theta_{N,o} = 0; \forall o \in O; \quad (33)$$

$$-\pi \leq \theta_{n,o} \leq \pi; \forall n \in \Lambda, o \in O; \quad (34)$$

$$0 \leq L_{n,o}^{\text{shed}} \leq \bar{f}_o^{\text{EL}} L_n; \forall n \in \Lambda, o \in O; \quad (35)$$

$$0 \leq P_{k,o}^{\text{GC}} \leq P_k^{\text{GC,INV}}; \forall k \in \Phi^{\text{GC}}, o \in O; \quad (36)$$

$$0 \leq P_{g,o}^{\text{GE}} \leq P_g^{\text{GE,max}}; \forall g \in \Phi^{\text{GE}}, o \in O; \quad (37)$$

$$0 \leq P_{j,o}^{\text{TC}} \leq P_j^{\text{TC,INV}}; \forall j \in \Phi^{\text{TC}}, o \in O; \quad (38)$$

$$0 \leq P_{i,o}^{\text{TE}} \leq P_i^{\text{TE,max}}; \forall i \in \Phi^{\text{TE}}, o \in O; \quad (39)$$

$$\begin{aligned} S_{p,o} - \bar{f}_o^{\text{GD}} D_p + D_p^{\text{shed}} - \sum_{g \in \Xi_p^{\text{GE}}} Q_{g,o}^{\text{GE}} - \sum_{k \in \Xi_p^{\text{GC}}} Q_{k,o}^{\text{GC}} \\ = \sum_{q \in \Xi_p} Q_{p,q,o} + \sum_{q \in \hat{\Xi}_p} \hat{Q}_{p,q,o}; \forall p \in \Xi, o \in O; \end{aligned} \quad (40)$$

$$0 \leq S_{p,o} \leq S_p^{\max}; \forall p \in \Xi, o \in O; \quad (41)$$

$$-\hat{Q}_{p,q}^{\text{INV}} \leq \hat{Q}_{p,q,o} \leq \hat{Q}_{p,q}^{\text{INV}}; \quad (42)$$

$$\forall p \in \Xi, q \in \hat{\Xi}_p, o \in O; \quad (43)$$

$$Q_{p,q}^{\max} \leq Q_{p,q,o} \leq Q_{p,q}^{\max}; \quad (44)$$

$$\forall p \in \Xi, q \in \Xi_p, o \in O; \quad (45)$$

$$0 \leq D_{p,o}^{\text{shed}} \leq \bar{f}_o^{\text{GD}} D_p; \forall p \in \Xi, o \in O; \quad (46)$$

$$Q_{k,o}^{\text{GC}} = b_k^{\text{GC}} P_{k,o}^{\text{GC}}; \forall k \in \Xi_p^{\text{GC}}, o \in O; \quad (47)$$

$$Q_{g,o}^{\text{GE}} = b_g^{\text{GE}} P_{g,o}^{\text{GE}}; \forall g \in \Xi_p^{\text{GE}}, o \in O. \quad (48)$$

This optimization model is the same as the one that is presented in Section II-B, with some notable differences in the objective function, variables, and constraints.

First, because this model is deterministic, objective function (24) minimizes total investment and operating costs. This can contrasted with objective function (1), which minimizes *expected* investment and operating costs.

Second, all of the first-stage planning variables that are in the model that is given in Section II-B appear in this deterministic model. Moreover, all of the operating variables in the two-stage stochastic optimization model have analogous variables in the deterministic model. However, none of the operating variables are indexed by scenario (ω) in the deterministic model. This is, again, because this model is deterministic.

Finally, the constraints in the deterministic model are all analogous to constraints in the stochastic model. Specifically, constraints (25)–(28) pertain to investment decisions and are analogous to constraints (2)–(5). Constraints (29)–(39) and (40)–(44) pertain to operation of the power and natural gas systems, respectively. Finally, constraints (45) and (46) con-

nect the power and natural gas systems through the fuel use of natural gas-fired units. These constraints are analogous to (6)–(16), (17)–(21), and (22) and (23), except that none of the constraints in the deterministic model are indexed by scenario (ω). This is because the deterministic model does not represent uncertainty. Instead, uncertain electricity and natural gas demands are replaced by their expected values, \bar{f}_o^{EL} and \bar{f}_o^{GD} , in constraints (29) and (40), respectively.

The VSS is computed by first solving this deterministic model to determine values of the first-stage investment variables (*i.e.*, $P_k^{\text{GC,INV}}$, $P_j^{\text{TC,INV}}$, $x_{m,n}$, and $\hat{Q}_{p,q}^{\text{INV}}$) if uncertainty is not taken into account in making planning decisions. These investment variables are fixed equal to the values that are obtained from the deterministic model, and the original two-stage stochastic planning model that is introduced in Section II-B is solved to determine the resulting second-stage operating decisions. We let z_D^* denote the optimal objective-function value of the two-stage stochastic planning model that is obtained by fixing the investment variables. We also let z_S^* denote the optimal objective-function value that is obtained from directly solving the two-stage investment model (*i.e.*, without fixing the investment decisions). The VSS is then defined as:

$$\frac{z_D^* - z_S^*}{z_S^*}.$$

III. ILLUSTRATIVE EXAMPLE

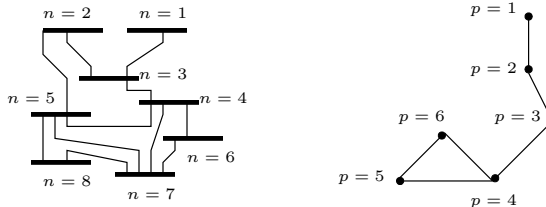
In this section we analyze a simple example based on an eight-zone model of the ISO New England system [2].

A. Data

This example is based on an eight-node model of the ISO New England power system¹ overlaid on a six-node natural gas system. Fig. 1a shows the topology of the power system. All eight of the nodes have electric loads and all nodes except for node 4 have existing or candidate units. Tables I and II summarize the characteristics of existing and candidate units, respectively, at each node, which are aggregations of existing and candidate units. Columns two and three of Table I specify the operating cost and maximum capacity, respectively, of the existing thermal unit at each power system node. The last three columns specify the natural gas node serving, the variable operation and maintenance cost of, and the maximum capacity of the existing natural gas-fired unit at each power system node. Columns two and three of Table II specify the operating and investment costs, respectively, of candidate thermal units at each power system node. The last three columns of the table specify the natural gas node serving and the operation and maintenance and investment costs of the candidate natural gas-fired unit at each power system node. We assume that a maximum of 1.5 GW of capacity of each candidate unit can be installed. Existing and candidate electricity transmission lines are assumed to have capacities of 1.5 GW. Each candidate line has an investment cost of \$45 million.

Fig. 1b shows the assumed topology of the natural gas system. There are two natural gas sources in the network (*i.e.*, two

¹<https://bitbucket.org/kdheepak89/eightbustestbedrepo/src/>



(a) Power system topology. (b) Natural gas system topology.

Fig. 1. Topology of ISO New England example.

TABLE I
 EXISTING-UNIT DATA FOR ISO NEW ENGLAND EXAMPLE

Power Node	Thermal Unit c_i^{TE}	Thermal Unit $P_i^{\text{TE,max}}$	Natural Gas-Fired Unit Gas Node	c_g^{GE}	$P_g^{\text{GE,max}}$
1	80	1050	1	4	2150
2	76	620	n/a	n/a	n/a
3	75	400	2	3	500
5	n/a	n/a	5	5	380
6	78	1100	3	4	1170
7	85	435	4	4	1840
8	88	2200	6	3	480

nodes have non-zero values of S_p^{max}). Node 1 of the natural gas system is connected to a large gas source while node 6 is connected to a relatively small one. Table III summarizes the existing capacity of the pipelines in the network. Up to 100000 MBTU/h of capacity can be added to each pipeline at a cost of \$100000/MBTU/h.

Electric and non-generation-related natural gas demands are modeled using historical data,²³ which are scaled based on the assumed generation and natural gas-pipeline capacities. Table IV summarizes the reference electric and non-generation-related natural gas loads for each power system and natural gas-system node. We assume a fixed natural gas price of \$3/MBTU at all nodes.

We generate 10 operating conditions, with different electric

²<http://iso-ne.com/isoexpress/web/reports/load-and-demand/-/tree/zone-info>
³https://www.eia.gov/dnav/ng/ng_cons_sum_a_EPG0_vgt_mmcfc_m.htm

TABLE II
 CANDIDATE-UNIT DATA FOR ISO NEW ENGLAND EXAMPLE

Power Node	Thermal Unit c_j^{TC}	Thermal Unit $C_j^{\text{T,INV}}$	Natural Gas-Fired Unit Gas Node	c_k^{GC}	$C_k^{\text{G,INV}}$
1	65	1300000	1	1	600000
2	72	1400000	n/a	n/a	n/a
3	55	1100000	2	2	700000
5	n/a	n/a	5	1	700000
6	70	1400000	3	3	900000
7	50	1000000	4	1	700000
8	60	1200000	6	2	800000

TABLE III
 NATURAL GAS PIPELINE DATA FOR ISO NEW ENGLAND EXAMPLE

p	q	$Q_{p,q}^{\text{max}}$
1	2	80000
2	3	70000
3	4	30000
4	5	20000
4	6	20000
5	6	20000

TABLE IV
 REFERENCE ELECTRIC AND NON-GENERATION-RELATED NATURAL GAS LOAD DATA FOR ISO NEW ENGLAND EXAMPLE

Power Node	L_n	Natural Gas Node	D_p
1	1337	1	5844
2	641	2	7668
3	1333	3	24767
4	2898	4	10376
5	1949	5	24767
6	1692	6	28352
7	927		
8	3501		

and non-generation-related natural gas loads. The different load levels are defined relative to the reference loads that are summarized in Table IV through the demand factors, $f_{\omega,o}^{\text{EL}}$ and $f_{\omega,o}^{\text{GD}}$. These demand factors are obtained by applying k -means clustering to historical data [19]. Table V summarizes the demand factors and weights on the 10 operating conditions obtained from the k -means clustering. The example in this section only assumes a single scenario (i.e., $|\Omega| = 1$).

TABLE V
 OPERATING-CONDITION DATA FOR ISO NEW ENGLAND EXAMPLE

o	$W_{\omega,o}$	$f_{\omega,o}^{\text{EL}}$	$f_{\omega,o}^{\text{GD}}$
1	941	1.2023	0.8173
2	543	0.9529	1.5282
3	1264	0.7840	0.9265
4	1487	1.0131	0.9406
5	873	1.2056	1.5345
6	949	0.7339	0.7710
7	478	1.0895	1.2982
8	416	1.4598	0.8418
9	1543	0.9754	0.7802
10	266	0.8656	1.2982

B. Results

Our example considers the following three cases to demonstrate how different investment costs affect planning decisions. The three cases are:

- Case 1, which uses the data that are summarized in Section III-A;
- Case 2, which is the same as Case 1, except that natural gas pipeline-investment costs are 50% lower; and
- Case 3, which is the same as Case 2, except that thermal unit investment costs are 20% greater.

Tables VI–VIII summarize the results of the example in the three cases. Table VI summarizes the total objective-function value and how it is broken down between investment and operating costs. Table VII lists unit investments. Power system nodes that are not listed do not have any investment in any of the cases. Table VIII summarizes investments in natural gas pipelines. Only three transmission lines are built in this example. Transmission lines connecting power system nodes 1 and 3 and nodes 3 and 4 are built in all three cases. A line connecting nodes 3 and 5 are built in Cases 2 and 3 only.

The tables show that among the three cases, Case 3 has the most investment in natural gas-fired units, least investments in thermal units, and lowest operational costs. Case 1 yields the opposite results. Although unit investments are driven by cost,

TABLE VI
OPTIMAL OBJECTIVE-FUNCTION VALUE IN ISO NEW ENGLAND
EXAMPLE

	Objective-Function Value [\$ billion]	Investment Cost [\$ billion]	Operating Cost [\$ billion]
Case 1	16.2	10.4	5.8
Case 2	15.2	9.52	5.6
Case 3	16.3	10.9	5.4

TABLE VII
UNIT-INVESTMENT DECISIONS IN ISO NEW ENGLAND EXAMPLE

Power Node	$P_j^{\text{TC,INV}}$	$P_k^{\text{GC,INV}}$		
		Case 1	Case 2	Case 3
1	0	0	0	1500
3	1500	1500	1500	1043
6	1500	921	0	0
7	1500	1500	1500	0
8	1500	1500	1500	0

there are competing interactions among thermal and natural gas-fired technologies. The candidate thermal unit at node 1 has lower investment and operating costs than the candidate thermal unit at node 6. Despite this, no thermal units are built at node 1. This is because node 1 also has the lowest-cost natural gas-fired unit. As such, the limited transmission capacity from node 1 to 3 (which is supplemented by building a transmission line connecting these two nodes) is dedicated to the existing unit at node 1 and natural gas-fired capacity that is built there. Thermal generation at node 6 is more costly than that at node 1 but less costly than other unbuilt thermal units. Thermal capacity is installed at node 6 (as opposed to node 1), because node 6 is subject to less transmission congestion than node 1 is.

Investments in natural gas-fired units may call for pipeline investments, which can significantly increase their overall cost. Thus, candidate natural gas-fired units that are close to fuel sources and require little pipeline investments are prioritized. This is the reason that the full 1.5 GW of candidate natural gas-fired capacity at power system node 1 is built in every case. The candidate natural gas-fired unit at this node is located at node 1 of the natural gas system, which is the larger of the two fuel sources. Thus, this unit uses *no* pipeline capacity. The candidate natural gas-fired unit at power system node 8 is located at node 6 of the natural gas system, which is the other fuel source. However, the natural gas source at this node is considerably smaller than the one at natural gas node 1. As such, no natural gas-fired units are built at power system node 8.

The candidate natural gas-fired unit at power system node 7 has lower investment and operating costs than the candidate natural gas-fired unit at node 6. Moreover, there is adequate pipeline capacity to node 4 of the natural gas system, where

the candidate unit at power system node 7 is located. As a result, natural gas-fired capacity is built at node 7 but not at node 6. Natural gas-fired units are not built at power system node 5, because of pipeline congestion and limited fuel supply from natural gas node 6.

The investment in natural gas-fired generation at power system node 3 (which is located at natural gas node 2) requires investments in a pipeline connecting natural gas nodes 1 and 2. Although this pipeline cost is high in Case 1, the candidate natural gas-fired unit at power system node 3 nevertheless represents a lower-cost alternative compared to the candidate thermal unit at power system node 2.

The candidate transmission line connecting power system nodes 3 and 5 is only built in Cases 2 and 3. This is to carry the added output of the candidate natural gas-fired unit at power system node 3 in these two cases.

This example is programmed using version 24.4.6 of the GAMS modeling language and solved using the hybrid branch-and-bound/cutting-plane algorithm with default settings in version 12.6.2.0 of the CPLEX mixed-integer linear program solver. The computations are conducted on a computer with a 2.6 GHz Intel Core i7 processor and 8 GB of RAM. The computation times of all three cases are approximately one minute.

IV. CASE STUDY

This section examines the proposed model using a modified IEEE 118-node test system⁴ and a 14-node natural gas system.

A. Data

The IEEE 118-node system is shown in Fig. 2 and the topology of the 14-node natural gas system is shown in Fig. 3. The IEEE 118-node system is divided into three zones. As the figure shows, there are limited transmission connections between the zones but relatively tight connections within each zone. Moreover, zones 1 and 2 are load pockets, in the sense that they have greater loads than available generating capacities, whereas zone 3 is a generation pocket. In total, the system has 91 load nodes, 21 generation nodes, and 186 transmission lines.

Two of the generation nodes have thermal units only while the others have both thermal and natural gas-fired units. Tables XVI and XVII, which are provided in the Appendix, summarize the existing and candidate units at the different power system nodes. The columns of these tables provide the same information for the case study that the columns of Tables I and II provide for the example. We assume that up to 1.5 GW of each candidate unit can be built. Candidate transmission lines can be built between nodes with existing lines. The capacity of each existing and candidate transmission line is 400 MW.

The natural gas system consists of 14 nodes that are connected by 13 existing pipelines, which are indicated by the solid lines in Fig. 3. All of nodes 2–12 have reference non-generation-related natural gas loads of 7200 MBTU/h.

⁴<http://www.ee.washington.edu/research/pstca/>

TABLE VIII
NATURAL GAS-PIPELINE-INVESTMENT DECISIONS IN ISO NEW ENGLAND EXAMPLE

p	q	Case 1	Case 2	Case 3
1	2	16475	22267	32261
2	3	0	0	9994

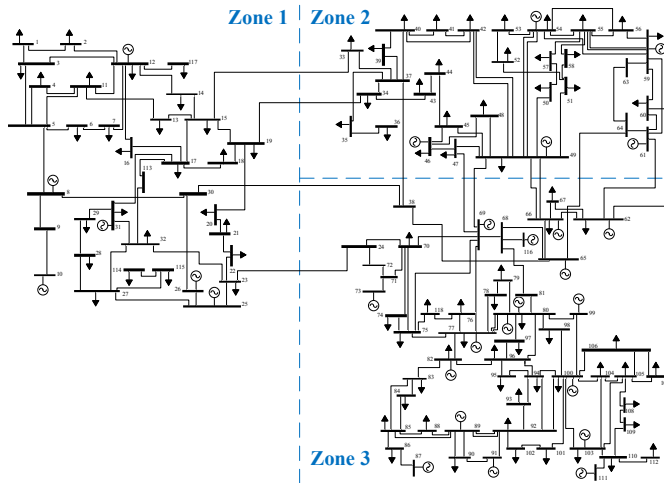


Fig. 2. Topology of IEEE 118-node test system.

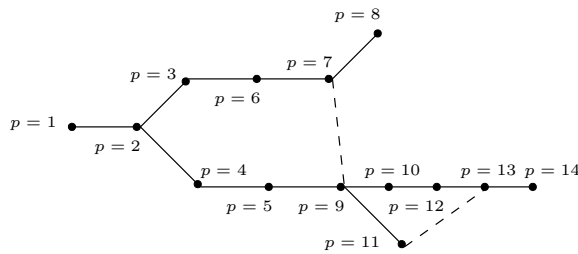


Fig. 3. Topology of 14-node natural gas system for IEEE 118-node test system.

There are two uncapacitated gas sources (*i.e.*, two nodes with $S_p^{\max} = +\infty$) at nodes 1 and 14. Table IX summarizes the capacities of the existing pipelines. Each existing pipeline can have up to 100000 MBTU/h of capacity added to it, at a cost of \$70000/MBTU/h. Fig. 3 also shows two non-existent candidate pipelines, which are indicated by the dotted lines. These two candidate pipelines can have up to 100000 MBTU/h of capacity installed at a cost of \$100000/MBTU/h. We assume a natural gas cost of \$4/MBTU at all nodes and under all scenarios and operating conditions.

TABLE IX
NATURAL GAS PIPELINE DATA FOR IEEE 118-NODE TEST SYSTEM

p	q	$Q_{p,q}^{\max}$	p	q	$Q_{p,q}^{\max}$	p	q	$Q_{p,q}^{\max}$
1	2	80000	2	4	35000	9	10	31000
2	3	45000	4	5	18000	10	12	42000
3	6	37000	5	9	10000	12	13	57000
6	7	24000	9	11	13500	13	14	65500
7	8	12000						

The reference electric load at each demand node of the power system is obtained from the work of Baringo [20]. We use the same 10 operating conditions as in the ISO New England case study, with the electricity and natural gas demand factors that are summarized in Table V. We further generate nine scenarios by scaling the natural gas and electric demand factors by the scaling factors that are given in Table X. Oftentimes scenarios that are input to a stochastic optimization problem are obtained from Monte Carlo simulation of the

underlying distributions of the random variables. For sake of simplicity, our case study assumes that electric and natural gas loads can differ by up to $\pm 10\%$ relative to the assumed baseline level. Given that our case study is intended to be a proof of concept for the proposed planning model, this is a reasonable assumption that introduces non-trivial uncertainties into the model. Table X summarizes the amount by which electricity and natural gas loads are scaled in each of the nine scenarios that are modeled.

TABLE X
SCENARIO DATA FOR IEEE 118-NODE TEST SYSTEM

ω	Scaling Factor		ω	Scaling Factor	
	Electric	Natural Gas		Electric	Natural Gas
1	1.0	1.0	6	1.0	0.9
2	0.9	0.9	7	1.0	1.1
3	1.1	1.1	8	0.9	1.0
4	0.9	1.1	9	1.1	1.0
5	1.1	0.9			

B. Results

We examine five cases with different investment costs and scenario probabilities. These five cases are:

- Case 1, which assumes the data that are summarized in Section IV-A and the probability vector:

$$\rho = (0.2, 0.1, 0.1, 0.1, 0.1, 0.1, 0.1, 0.1, 0.1);$$

- Case 2, which is the same as Case 1, except that natural gas pipeline-investment costs are 20% lower;
- Case 3, which is the same as Case 1, except that natural gas-fired unit-investment costs are 20% lower;
- Case 4, which is the same as Case 1, except that power system transmission-investment costs are 100% higher; and
- Case 5, which is the same as Case 1, except that the probability vector is:

$$\rho = (0.05, 0.05, 0.25, 0.05, 0.2, 0.05, 0.05, 0.05, 0.25).$$

Table XI–XIV summarize investments in thermal units, natural gas-fired units, transmission lines, and natural gas pipelines, respectively, in the five cases considered. As expected, natural gas-fired units are only built at power system nodes that are close to fuel sources, reducing the need for pipeline investments.

TABLE XI
THERMAL UNIT-INVESTMENT DECISIONS IN IEEE 118-NODE TEST SYSTEM [MW]

Power Node	Case 1	Case 2	Case 3	Case 4	Case 5
12	0	0	0	19	0
26	116	257	251	213	235
31	0	0	0	323	0
46	1049	275	244	1073	533
59	54	220	222	311	174
65	1319	1177	1129	652	1500

All of the cases result in roughly the same amount of total generating capacity investment—Case 2 has the least

TABLE XII
NATURAL GAS-FIRED UNIT-INVESTMENT DECISIONS IN IEEE 118-NODE TEST SYSTEM [MW]

Power Node	Case 1	Case 2	Case 3	Case 4	Case 5
10	193	193	193	182	193
100	0	0	39	0	0
103	0	0	108	0	0
111	175	752	752	133	271

TABLE XIII
TRANSMISSION LINE-INVESTMENT DECISIONS IN IEEE 118-NODE TEST SYSTEM

<i>n</i>	<i>m</i>	Case 1	Case 2	Case 3	Case 4	Case 5
5	8	1	1	1	1	1
8	9	1	1	1	1	1
9	10	1	1	1	1	1
17	30	1	1	1	0	1
37	38	1	1	1	0	1
38	65	1	1	1	0	1
64	65	1	1	1	0	1
110	111	0	1	1	0	0

investment at 2874 MW while Case 3 has the most at 2938 MW. The breakdown of the generation mix differs among the cases, however. Case 2 results in more natural gas-fired units being built compared to Case 1. This is because of the lower pipeline-investment cost in Case 2. Considerably more capacity is added to the pipeline connecting natural gas nodes 11 and 13 in Case 2 (compared to Case 1) to accommodate greater production from the existing natural gas-fired unit at power system node 89, which is connected to natural gas node 11. Case 2 has less *total* generating capacity investment, because the reduced pipeline-investment costs allow for greater use of existing natural gas-fired units. Case 1, conversely, sees more thermal units being built to serve load, because relying on natural gas-fired units is relatively costly. Case 2 also sees investment in the transmission line connecting nodes 110 and 111, because of investment in a candidate natural gas-fired unit at power system node 111. This line is not built in Case 1.

Case 3 also sees greater total investment in generating capacity and in natural gas-fired units compared to Case 1. This is driven by the reduced investment costs of natural gas-fired units, which results in partially unused capacity being built. For instance, 108 MW of natural gas-fired capacity is installed at power system node 103. However, this candidate unit produces below 108 MW in a number of operating conditions with low electric loads. This phenomenon of building

capacity that goes unused does not occur in Cases 1 and 2 because of the relatively high investment cost of generating units. Rather, in Cases 1 and 2 all of the added natural gas-fired capacity operates at its installed nameplate capacity under all operating conditions. Production of existing natural gas-fired units is lower in Case 3 compared to Cases 1 and 2. The pipeline connecting natural gas nodes 10 and 12 is also not expanded in Case 3 because of the reduced use of existing natural gas-fired units.

Case 4 has the same amount of total generating capacity added that Case 1 does. The units built in Case 4 are chosen, however, to minimize the need for transmission capacity, due to the higher transmission-investment costs. Thermal units are built at power system nodes 12 and 31 and there is less investment in the thermal unit at node 26 (compared to Case 1) to avoid construction of the transmission line connecting nodes 17 and 30. Similarly, less generating capacity is built at power system node 65 to avoid construction of transmission lines connecting nodes 38 and 64 to node 65. Instead, capacity is built at power system nodes 46 and 59 to serve electric loads in zone 2 of the transmission network. There is also less investment in natural gas-fired generation at power system node 111 to avoid construction of a transmission line between nodes 110 and 111.

Case 5 results in greater investment in natural gas-fired units to accommodate the greater probability of scenarios with high electric loads (*i.e.*, ρ_3 , ρ_5 , and ρ_9 are greater in Case 5 than Case 1). This is because natural gas-fired units have relatively low operating costs compared to thermal units, giving them a cost advantage in high-load scenarios. Total generation investments are the same in the two cases.

As in the example that is examined in Section III, there are interesting interactions in which candidate generating units are built. For instance, in all but Case 4, the thermal unit at power system node 65 has the highest priority to be built, due to its relatively low cost. Significantly less thermal capacity is built at node 65 in Case 4, however, because of the high transmission-investment costs. In its place, thermal capacity is built at node 46 in Case 4. As another example, zone 2 of the power system, which contains nodes 46 and 59, has greater electric loads than existing generation. Most of the load in zone 2 is served by either thermal investments at power system node 46 (in Cases 1 and 4) or by a combination of investments in thermal units at nodes 46, 59, and 65 and natural gas-fired capacity at node 111 (in the other three cases). Thermal capacity is built at node 59 in all five cases (even though it is more costly than capacity at node 46) to avoid building two transmission lines connecting node 59 to 64 via node 63. Cases in which there is less generating capacity built at node 46 (*i.e.*, Cases 2, 3, and 5) require greater investments in generating capacity at node 26 to serve electric loads in zone 1.

Table XV summarizes the results of conducting VSS calculations in the five cases, assuming load-curtailment costs of $V^{LL,E} = 15400$ and $V^{LL,G} = 1400$. The stochastic planning model does not yield any electricity or natural gas curtailment for curtailment costs above these values. However, the investment decisions made by the deterministic model that is given in Section II-C does result in both electricity and

TABLE XIV
NATURAL GAS PIPELINE-INVESTMENT DECISIONS IN IEEE 118-NODE TEST SYSTEM

<i>p</i>	<i>q</i>	Case 1	Case 2	Case 3	Case 4	Case 5
1	2	23746	23746	23746	23651	23746
2	3	5000	5000	5000	5000	5000
6	7	306	306	306	306	306
7	8	153	153	153	153	153
2	4	400	400	400	400	400
10	12	350	350	0	350	350
13	14	5970	11524	12138	5596	6836
11	13	0	355	0	0	0

natural gas curtailments. This is because the investment levels are determined to meet expected load levels, which does not take into account the possibility of high load levels in some scenarios. These load curtailments yield the high VSSs that are reported in the second column of the table.

TABLE XV
RESULTS OF VALUE OF STOCHASTIC SOLUTION COMPUTATIONS IN IEEE 118-NODE TEST SYSTEM

Case	VSS [%]	Expected Curtailment With Investments From Deterministic Planning Model	
		Electricity [MWh]	Natural Gas [MBTU]
1	53.98	369219	1713469
2	58.88	369643	1708810
3	53.90	372450	1677936
4	52.70	369219	1713469
5	67.94	408029	1905977

The third and fourth columns of Table XV report the expected electricity and natural gas curtailments, respectively. These columns show that load curtailments can be substantial, which explains the high VSSs that are reported in the second column.

The case studies presented here are all implemented in the same computing environment that is used for the example in Section III. The computation time of all five cases is about one hour.

V. CONCLUSIONS

As natural gas-fired units increasingly dominate the generation portfolio of electric power systems, joint coordination of natural gas and power systems is a must. This increasingly includes coordinating long-term expansion planning of the two systems. This paper provides a modeling approach that does such joint coordination and considers uncertainties in electricity- and natural gas-demand growth. Modeling of such uncertainties within a planning model is a novelty relative to the existing literature. The model structure can also easily be adapted to include other types or sources of uncertainties. This can include short-run uncertainties, such as variable resource availability from renewable generators, or long-run uncertainties, such as policy or technology changes. Because our focus here is on studying interactions between natural gas and electricity systems, we limit our analysis to modeling uncertainties in electricity and natural gas demand-growth rates.

A benefit of the model that we develop is that it allows quantitatively assessing the long-term implications of increasingly relying on natural gas-fired generation units. Conversely, the model also allows examining the alternate implications of increasingly relying on other generation technologies. Increasingly relying on natural gas-fired generators requires expanding the natural gas-pipeline infrastructure and, to a lesser extent, the electricity transmission grid. Indeed, one of the trade-offs that our model, example, and case study reveal is that energy can either be moved in the network in a 'raw' form via natural gas pipelines or in a 'complete' form via transmission lines. Uncertainty in the future availability of natural gas has a significant impact on the overall expansion

exercise. This, in turn, alters the trade-offs in building natural gas-fired units, other generation technologies, natural gas pipeline infrastructure, and electricity transmission lines. The joint coordination that our model captures allows these trade-offs to be examined closely.

We employ a static investment that consists of a set of initial first-stage investment decisions, followed by second-stage operating decisions. One could expand our modeling framework to allow for multiple planning stages [17]. Conversely, the model that we proposed could also be applied in a rolling-horizon fashion to update investment decisions as uncertainties are revealed. We also employ a linearized model of the natural gas system, representing flows as in a transportation network. One could embed dynamic nonlinear flows within our proposed modeling framework. However, doing so would raise serious computational challenges as the resulting model would be a mixed-integer nonlinear stochastic problem. We leave such a model for future research. Nevertheless, we do not expect the qualitative findings of our model, example, and case study to be drastically affected by nonlinear flows.

We demonstrate the value of using a stochastic planning model by examining the VSS. Our results show that a deterministic model can result in underbuilding the system, because it plans against expected demand levels. This points to the need for heuristic workarounds if a deterministic planning model is used. For instance, planning reserve margins or similar types of constraints can be added to a deterministic planning model to ensure that sufficient capacity (to meet potential high demand-growth rates) is built. The fact that our stochastic planning model does not result in any load curtailment shows a benefit of explicitly representing demand uncertainty.

APPENDIX UNIT DATA FOR IEEE 118-NODE TEST SYSTEM

Assumed characteristics of existing and candidate units in the case study that is examined in Section IV are provided here.

ACKNOWLEDGMENT

Thank you to Armin Sorooshian, the editors, and five reviewers for helpful suggestions, comments, and conversations.

REFERENCES

- [1] *Phase 2 Report: Interregional Transmission Development and Analysis for Three Stakeholder Selected Scenarios And Gas-Electric System Interface Study*, Eastern Interconnection Planning Collaborative, 2 July 2015.
- [2] D. Krishnamurthy, W. Li, and L. Tesfatsion, "An 8-Zone Test System Based on ISO New England Data: Development and Application," *IEEE Transactions on Power Systems*, vol. 31, pp. 234–246, January 2016.
- [3] C. Unsihuay-Vila, J. W. Marangon-Lima, A. C. Zambroni de Souza, I. J. Perez-Arriaga, and P. P. Balestrassi, "A Model to Long-Term, Multiarea, Multistage, and Integrated Expansion Planning of Electricity and Natural Gas Systems," *IEEE Transactions on Power Systems*, vol. 25, pp. 1154–1168, May 2010.
- [4] J. Qiu, H. Yang, Z. Y. Dong, J. H. Zhao, K. Meng, F. J. Luo, and K. P. Wong, "A Linear Programming Approach to Expansion Co-Planning in Gas and Electricity Markets," *IEEE Transactions on Power Systems*, vol. 31, pp. 3594–3606, September 2016.

TABLE XVI
EXISTING-UNIT DATA FOR IEEE 118-NODE TEST SYSTEM

Power Node	Thermal Unit	Natural Gas-Fired Unit			
	c_i^{TE}	$P_i^{\text{TE,max}}$	Gas Node	c_g^{GE}	$P_g^{\text{GE,max}}$
10	88	202	2	5	405
12	89	38	3	3	77
25	90	99	4	6	198
26	84	96	4	5	279
31	86	4	5	6	8
46	81	9	6	3	18
49	82	92	6	3	184
54	80	22	7	3	43
59	84	70	8	5	140
61	85	72	8	3	144
65	86	176	9	4	353
66	89	176	9	3	353
69	90	232	9	6	464
73	89	50	n/a	n/a	n/a
80	84	215	10	3	430
87	86	2	11	5	9
89	81	273	11	4	547
100	82	113	12	4	227
103	80	18	13	3	36
111	84	16	13	4	32
116	87	75	n/a	n/a	n/a

TABLE XVII
CANDIDATE-UNIT DATA FOR IEEE 118-NODE TEST SYSTEM

Power Node	Thermal Unit	Natural Gas-Fired Unit			
	c_j^{TC}	$C_j^{\text{T,INV}}$	Gas Node	c_k^{GC}	$C_k^{\text{G,INV}}$
10	80	1920000	2	3	1400000
12	82	1968000	3	2	1350000
25	83	1999200	4	4	1450000
26	75	1800000	4	3	1400000
31	77	1848000	5	4	1450000
46	72	1728000	6	2	1350000
49	74	1776000	6	2	1350000
54	76	1824000	7	2	1350000
59	73	1752000	8	4	1450000
61	75	1800000	8	2	1350000
65	70	1680000	9	3	1400000
66	82	1968000	9	1	1300000
69	83	1992000	9	4	1450000
73	83	1992000	n/a	n/a	n/a
80	75	1800000	10	2	1350000
87	77	1848000	11	3	1400000
89	72	1728000	11	3	1400000
100	74	1776000	12	2	1350000
103	76	1824000	13	4	1450000
111	74	1752000	13	2	1350000
116	82	1968000	n/a	n/a	n/a

- [5] C. A. Saldarriaga, R. A. Hincapié, and H. Salazar, "A Holistic Approach for Planning Natural Gas and Electricity Distribution Networks," *IEEE Transactions on Power Systems*, vol. 28, pp. 4052–4063, November 2013.
- [6] J. Qiu, Z. Y. Dong, J. H. Zhao, Y. Xu, Y. Zheng, C. Li, and K. P. Wong, "Multi-Stage Flexible Expansion Co-Planning Under Uncertainties in a Combined Electricity and Gas Market," *IEEE Transactions on Power Systems*, vol. 30, pp. 2119–2129, July 2015.
- [7] F. Barati, H. Seifi, M. S. Sepasian, A. Nateghi, M. Shafie-khah, and J. P. S. Catalão, "Multi-Period Integrated Framework of Generation, Transmission, and Natural Gas Grid Expansion Planning for Large-Scale Systems," *IEEE Transactions on Power Systems*, vol. 30, pp. 2527–2537, September 2015.
- [8] X. Zhang, M. Shahidehpour, A. S. Alabdulwahab, and A. Abusorrah, "Security-Constrained Co-Optimization Planning of Electricity and Natural Gas Transportation Infrastructures," *IEEE Transactions on Power Systems*, vol. 30, pp. 2984–2993, November 2015.
- [9] M. Chaudry, N. Jenkins, M. Qadrdan, and J. Wu, "Combined gas and electricity network expansion planning," *Applied Energy*, vol. 113, pp. 1171–1187, January 2014.

- [10] J. Qiu, Z. Y. Dong, J. H. Zhao, K. Meng, Y. Zheng, and D. J. Hill, "Low Carbon Oriented Expansion Planning of Integrated Gas and Power Systems," *IEEE Transactions on Power Systems*, vol. 30, pp. 1035–1046, March 2015.
- [11] D. Wang, J. Qiu, K. Meng, X. Gao, and Z. Dong, "Coordinated expansion co-planning of integrated gas and power systems," *Journal of Modern Power Systems and Clean Energy*, vol. 5, pp. 314–325, May 2017.
- [12] S. Jin and S. M. Ryan, "Capacity Expansion in the Integrated Supply Network for an Electricity Market," *IEEE Transactions on Power Systems*, vol. 26, pp. 2275–2284, November 2011.
- [13] I. Sharan and R. Balasubramanian, "Integrated generation and transmission expansion planning including power and fuel transportation constraints," *Energy Policy*, vol. 43, pp. 275–284, April 2012.
- [14] J. E. Bistline, "Natural gas, uncertainty, and climate policy in the US electric power sector," *Energy Policy*, vol. 74, pp. 433–442, November 2014.
- [15] —, "Electric sector capacity planning under uncertainty: Climate policy and natural gas in the US," *Energy Economics*, vol. 51, pp. 236–251, September 2015.
- [16] A. J. Conejo, L. B. Morales, S. J. Kazempour, and A. S. Siddiqui, *Investment in Electricity Generation and Transmission: Decision Making under Uncertainty*. Cham, Switzerland: Springer International Publishing, 2016, vol. 205.
- [17] Y. Liu, R. Sioshansi, and A. J. Conejo, "Multistage Stochastic Investment Planning with Multiscale Representation of Uncertainties and Decisions," *IEEE Transactions on Power Systems*, 2017, in press.
- [18] A. J. Conejo, M. Carrión, and J. M. Morales, *Decision Making Under Uncertainty in Electricity Markets*, ser. International Series in Operations Research & Management Science. New York, New York: Springer Science+Business Media, LLC, 2010, vol. 153.
- [19] L. Baringo and A. J. Conejo, "Correlated wind-power production and electric load scenarios for investment decisions," *Applied Energy*, vol. 101, pp. 475–482, January 2013.
- [20] L. Baringo, "Stochastic Complementarity Models for Investment in Wind-Power and Transmission Facilities," Ph.D. dissertation, Universidad de Castilla-La Mancha, Ciudad Real, Spain, October 2013.



Bining Zhao received the B.S. degree in electrical engineering and automation from North China Electric Power University, Baoding, China, in 2014. She is currently working toward her Ph.D. degree in the Department of Electrical and Computer Engineering at The Ohio State University, Columbus, OH.



Antonio J. Conejo (F'04) received the M.S. degree from the Massachusetts Institute of Technology, Cambridge, MA, in 1987, and the Ph.D. degree from the Royal Institute of Technology, Stockholm, Sweden, in 1990.

He is currently a professor in the Department of Integrated Systems Engineering and the Department of Electrical and Computer Engineering, The Ohio State University, Columbus, OH. His research interests include control, operations, planning, economics and regulation of electric energy systems, as well as statistics and optimization theory and its applications.



Ramteen Sioshansi (M'11–SM'12) holds the B.A. degree in economics and applied mathematics and the M.S. and Ph.D. degrees in industrial engineering and operations research from the University of California, Berkeley, and an M.Sc. in econometrics and mathematical economics from The London School of Economics and Political Science.

He is an associate professor in the Department of Integrated Systems Engineering at The Ohio State University, Columbus, OH. His research focuses on renewable and sustainable energy system analysis and the design of restructured competitive electricity markets.